Development and Characterization of Antifungal Nanoemulsions for Topical Drug Delivery

Sachin Kumar, Ms. Aarti Kori, Dr. Shivanand Patil

Abstract:

This study aimed to develop and optimize a luliconazole-loaded nanoemulgel for enhanced topical antifungal delivery, addressing the challenges of poor solubility and skin permeation associated with conventional formulations. A Design of Experiments (DoE) approach was employed, utilizing a Box-Behnken Design (BBD) to optimize critical formulation parameters, including oil concentration (5–15% v/v), surfactant mixture (Smix) ratio (15–45% v/v), and sonication time (5–15 min). Clove oil was selected as the oil phase due to its superior solubility for luliconazole (775 ± 0.14 µg/mL), while Tween 80 and Transcutol P were chosen as surfactants based on phase behavior studies.

The optimized nanoemulgel exhibited a nanoscale globule size (130.5 ± 3.23 nm), low polydispersity index (PDI: 0.263 ± 2.67), and high entrapment efficiency (80 ± 1.43%). Zeta potential (-21 ± 2.35 mV) and TEM imaging confirmed colloidal stability and spherical morphology. The formulation demonstrated pH compatibility (6.8 ± 2.25), excellent spreadability (13 ± 2.43 g·cm/sec), and pseudoplastic rheological behavior, ensuring ease of application and sustained drug release.

In vitro release studies revealed 74.93 ± 0.8% drug release over 8 hours, following Higuchi kinetics (R^2 = 0.9828), indicative of a diffusion-controlled mechanism. FTIR analysis confirmed the absence of drug-excipient incompatibilities, preserving luliconazole's structural integrity. Stability studies indicated robust physical and chemical stability under varied storage conditions.

The developed luliconazole nanoemulgel offers a promising topical antifungal delivery system, enhancing solubility, skin permeation, and sustained release, with potential applications in treating superficial fungal infections.

Keywords: Nanoemulgel, Luliconazole, Topical delivery, Antifungal, Design of Experiments (DoE), Box-Behnken Design, Higuchi kinetics, Transcutol P, Clove oil

Introduction

Topical Drug Delivery Systems

Pharmaceutical agents are most commonly administered via oral, intravenous, subcutaneous, or topical routes. Among these, topical delivery systems (TDSs) have gained prominence for their ability to provide sustained drug release over extended periods, ranging from hours to days, particularly when formulated as adhesive patches [1]. These systems are especially advantageous for drugs with short plasma half-lives, as they enable localized delivery directly to target tissues, bypassing systemic circulation. This targeted approach minimizes systemic side effects and enhances therapeutic efficacy, making TDSs particularly valuable in pain management [2–4]. Unlike systemic analgesics, which can cause adverse effects and dependency [5–8], topical formulations offer site-specific action, reduced dosing requirements, and avoidance of first-pass metabolism [2,4,9].

The absorption and penetration of drugs through skin layers—stratum corneum, epidermis, dermis, and subcutaneous adipose tissue (SAT)—into deeper muscle tissues are influenced by factors such as molecular size, lipophilicity, and protein-binding affinity [10–12]. While capillary networks in these tissues can facilitate systemic redistribution [13], the relative contributions of direct diffusion versus systemic uptake to local drug efficacy remain incompletely understood [14]. Clinicians frequently employ adhesive TDSs (commonly called patches or plasters) containing lidocaine for musculoskeletal and neuropathic pain, such as lower back pain [2,3,15]. These systems are designed to deliver the drug directly to superficial muscle tissue, providing localized relief [16,17]. However, a common misconception is that higher drug concentrations in TDSs correlate with greater efficacy. In reality, the labeled drug percentage reflects the drug-to-adhesive ratio rather than the actual dose delivered to target tissues [11]. Further research is needed to quantify the proportion of drug released from TDSs that reaches muscle tissue via diffusion or systemic redistribution, as this will inform optimal patch placement and design.

Nanoemulsions: Evolution, Properties, and Pharmaceutical Applications

Nanoemulsions have emerged as one of the most promising colloidal drug delivery systems in modern pharmaceutical science, representing a significant advancement over conventional emulsion technologies. These thermodynamically stable systems consist of two immiscible liquids (typically oil and water) stabilized by an interfacial film of surfactant molecules, with droplet sizes characteristically in the nanometer range (20-200 nm). The historical development of nanoemulsions traces back to the early 20th century when scientists first began exploring colloidal systems, though the term "nanoemulsion" gained widespread acceptance only in the 1990s as nanotechnology

advanced. Unlike microemulsions which are thermodynamically stable but require high surfactant concentrations, nanoemulsions exhibit kinetic stability with relatively lower surfactant requirements, making them more pharmaceutically viable. The unique properties of nanoemulsions stem from their nanoscale droplet size, including optical transparency, high surface area, and tunable rheological behavior, which collectively contribute to their growing importance in drug delivery applications.

The fundamental properties of nanoemulsions that make them particularly valuable for pharmaceutical applications include their exceptional stability against sedimentation or creaming, ability to incorporate both hydrophilic and lipophilic drugs, and capacity to enhance drug solubility and bioavailability. From a physicochemical perspective, nanoemulsions demonstrate Brownian motion that prevents droplet aggregation, with their stability further enhanced by electrostatic or steric repulsion between droplets depending on the surfactant system employed. The optical clarity of nanoemulsions, resulting from droplet sizes smaller than the wavelength of visible light, provides aesthetic advantages for certain pharmaceutical products. Rheologically, nanoemulsions can be formulated to exhibit Newtonian or non-Newtonian flow properties depending on composition and droplet concentration, allowing customization for various administration routes. The large interfacial area of nanoemulsions (approximately 50-100 m^2/g) facilitates rapid drug release and enhanced absorption, while their nanoscale dimensions promote tissue penetration and cellular uptake.

The preparation of pharmaceutical-grade nanoemulsions involves several well-established techniques that can be broadly categorized as high-energy or low-energy methods. High-energy approaches utilize mechanical devices such as high-pressure homogenizers, microfluidizers, or ultrasonicators to disrupt the oil and water phases into nanodroplets, requiring significant energy input but offering better control over droplet size distribution. Low-energy methods, including phase inversion temperature (PIT) and emulsion inversion point (EIP) techniques, rely on the spontaneous formation of nanoemulsions through careful manipulation of system composition and environmental parameters. The selection of appropriate components - oils (long-chain triglycerides, medium-chain triglycerides, or specialty oils), surfactants (ionic, nonionic, or zwitterionic), and cosurfactants (short-chain alcohols or polyols) - critically determines the final characteristics and stability of the nanoemulsion system. Recent advances in nanoemulsion fabrication have introduced more sophisticated techniques such as membrane emulsification and microfluidic production, enabling precise control over droplet size and monodispersity for specialized applications.

In pharmaceutical sciences, nanoemulsions have demonstrated remarkable versatility across multiple administration routes, each offering unique advantages. For oral delivery, nanoemulsions enhance the

bioavailability of poorly water-soluble drugs by maintaining them in solubilized form throughout the gastrointestinal tract, while also potentially reducing inter-subject variability and food effects. Parenteral nanoemulsions, particularly those based on lipid compositions similar to natural chylomicrons, can serve as efficient carriers for intravenous drug delivery, with several products already marketed for parenteral nutrition and anesthetic delivery. Transdermal nanoemulsions facilitate skin permeation through multiple mechanisms including hydration effects, disruption of stratum corneum lipids, and follicular targeting, making them valuable for both local and systemic delivery. Ophthalmic nanoemulsions provide sustained drug release and improved corneal penetration while minimizing irritation, addressing significant challenges in treating anterior and posterior segment eye diseases. Additionally, pulmonary nanoemulsions show promise for targeted lung delivery, with their small droplet size facilitating deep alveolar deposition when administered via nebulization.

Material & Methods

1. **Active Pharmaceutical Ingredient (API):**
   - **Antifungal agent(s)** Luliconazole
2. **Oils:**
   - **Oil phase:** Medium-chain triglycerides (MCT), *Caprylic/Capric Triglycerides*, *Soybean oil*, *Castor oil*, etc.
   - **Essential oils (optional) for added antifungal or soothing effects.**
3. **Surfactants:**
   - Nonionic surfactants such as *Tween 80* (Polysorbate 80), *Tween 20*, or *Pluronic F-68* for stabilization.
   - **Co-surfactants:** *Ethanol*, *Propylene Glycol*, or *Glycerol* may be used to improve solubility and stability.
4. **Water Phase:**
   - **Purified water or *Phosphate-buffered saline (PBS)*.**
5. **Stabilizers/Preservatives (Optional):**
   - **Such as *Vitamin E* for stability or *Sodium Chloride* for tonicity adjustments.**

Methods:

1. Formulation of Nano emulsion:

a) Preformulation Studies:

- **Solubility testing:** Test the solubility of the antifungal agent in various oils and surfactants to identify suitable solvents.
- **Phase Diagram Construction:** Prepare pseudoternary phase diagrams (using oil, surfactant, co-surfactant, and water) to determine the optimum surfactant-to-oil ratio.

b) Nano emulsion Preparation (Emulsification Process):

- **High Shear Homogenization Method:**

1. **Oil Phase Preparation:** Dissolve the antifungal agent in the oil phase.
2. **Surfactant Phase:** Mix the surfactant and co-surfactant in water and heat to an appropriate temperature (e.g., 70–80°C).
3. **Emulsification Process:** Add the oil phase into the surfactant phase under continuous stirring or high shear homogenization (e.g., using an Ultra-Turrax, or homogenizer) to form the nano emulsion.
4. **Cooling and Storage:** Allow the nano emulsion to cool to room temperature and store it in a tightly sealed container, protected from light, at appropriate storage conditions (e.g., 4–25°C).

Low Energy Emulsification (Spontaneous Emulsification):

5. Mix the oil, surfactant, and co-surfactant.
6. Slowly add water under stirring, inducing spontaneous emulsification.
7. After emulsification, allow the nano emulsion to stabilize.

2. Characterization of Nanoemulsion:

a) Visual Inspection:

Check for phase separation, turbidity, and clarity. A homogeneous, translucent solution indicates successful emulsification.

b) Particle Size, Polydispersity Index (PDI), and Zeta Potential:

Dynamic Light Scattering (DLS): Use DLS to determine particle size distribution and PDI, ensuring a nano range (typically 50–500 nm).

- **Zeta Potential Measurement:** Measure the zeta potential using a Zetasizer, which provides an indication of the stability of the nanoemulsion (a zeta potential greater than ±30 mV typically indicates good stability).

c) pH and Viscosity:

- Measure the pH of the formulation using a pH meter to ensure it is suitable for topical application (typically pH 4–7).
- **Viscosity Measurement:** Use a Brookfield viscometer to measure viscosity. The viscosity will indicate the ease of application and spreadability.

d) Stability Studies:

- **Thermal Stability:** Store the nanoemulsion at different temperatures (e.g., 4°C, 25°C, and 40°C) and evaluate for any physical changes (e.g., phase separation or cloudiness) over time.
- **Centrifugation:** Conduct centrifugation studies (e.g., 10,000 rpm for 30 minutes) to check the physical stability and resistance to separation.

e) Drug Content Analysis:

- **UV-Vis Spectrophotometry:** Measure the drug concentration in the nanoemulsion by UV spectroscopy at the specific wavelength of the antifungal drug.
- HPLC or HPTLC (High-performance Thin Layer Chromatography) can be used for more precise quantification.

3. Release Kinetics:

- Perform In Vitro Release Studies using dialysis membrane or Franz diffusion cells to evaluate the release rate of the antifungal agent.
- **Modeling:** Analyze the data using kinetic models such as zero-order, first-order, Higuchi, or Korsmeyer-Peppas to understand the release mechanism.

Result & Discussion

Solubility assessment of luliconazole

The solubility evaluation of Luliconazole was conducted in multiple vegetable oils, with clove oil exhibiting the highest solubility at 775±0.14 µg/ml. The findings indicated that Luliconazole has significantly greater solubility in clove oil compared to other oils. Previous research supports the use of clove oil as a suitable vegetable oil for producing clear nanoemulsions [11]. The current study further revealed that Luliconazole nanosuspensions show improved solubility in clove oil, surpassing results from earlier research [12]. The solubility data for Luliconazole in various vegetable oils are presented in Table 4, with a comparative analysis illustrated in Figure 1.

Table 4: Solubility of Luliconazole in Different Vegetable Oils

S. No.	Vegetable Oil	Solubility (µg/ml, Mean ± SD)
1	Castor oil	44 ± 0.22
2	**Clove oil**	**775 ± 0.14**
3	Oleic acid	104 ± 0.23
4	Eucalyptus oil	148 ± 0.36
5	Olive oil	32 ± 0.15

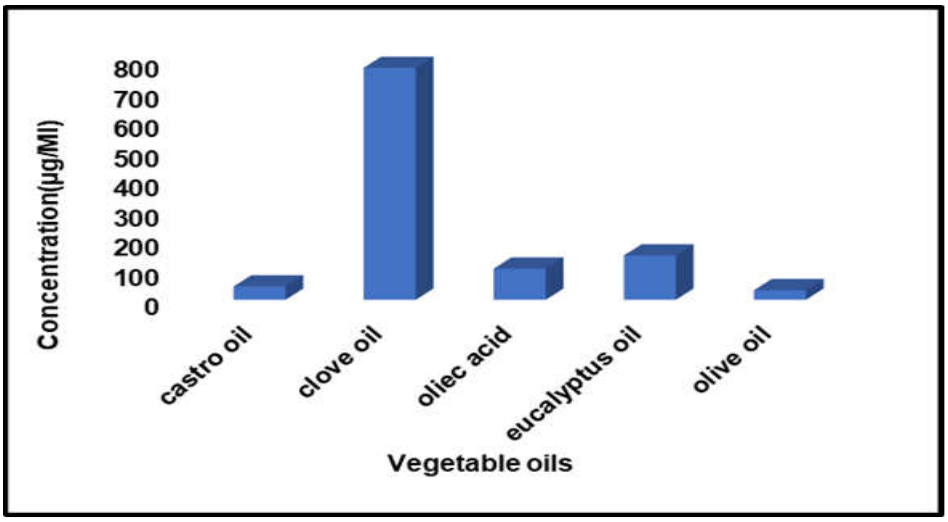

Fig. 1: Solubility of luliconazole in different vegetable oils, the results are given in mean

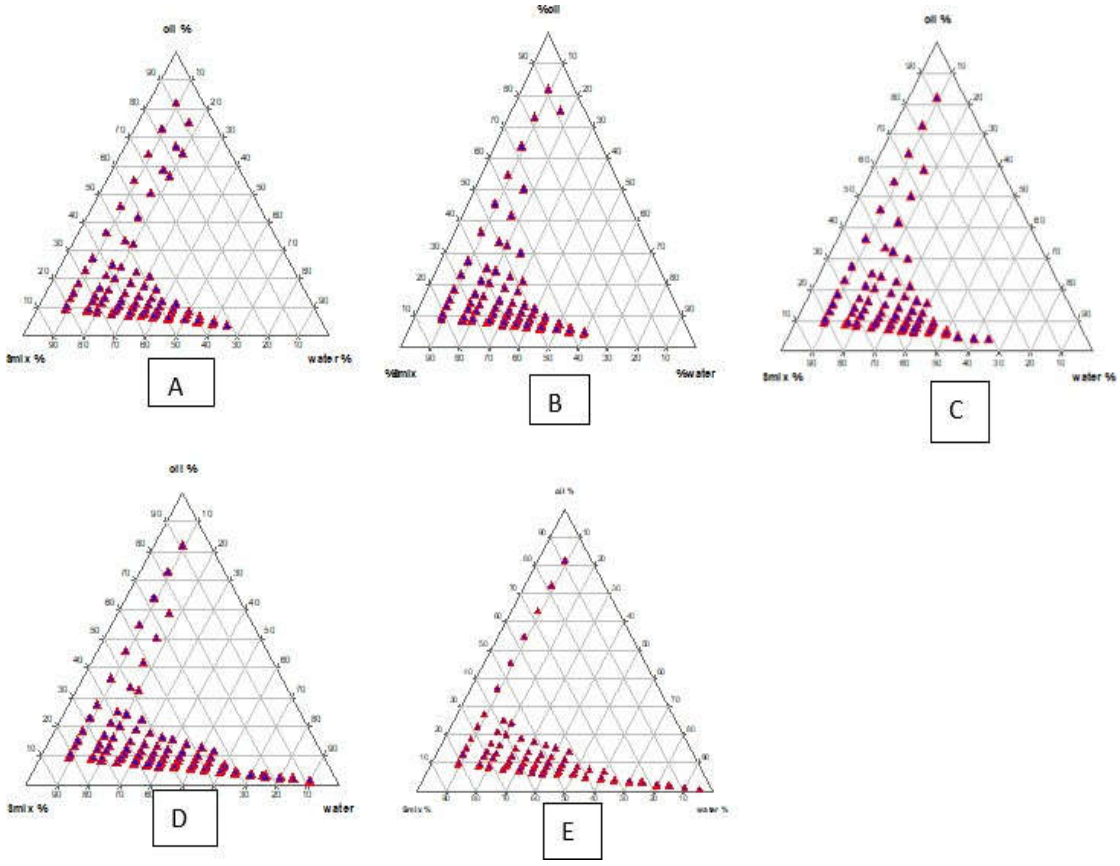

Fig. 2: Ternary phase diagrams of smix ratio (tween 80: transcutol P) A(1:1), B(1:2), C(1:3), D (2:1), E(3:1)

Oil Emulsification Studies

The emulsification capability of surfactants plays a crucial role in formulating stable nanoemulsions. In this study, different surfactants were evaluated for their oil-emulsifying efficiency. Since a blend of lipophilic and hydrophilic surfactants is essential for nanoemulsion stability, Tween 80 and Transcutol P were tested at varying ratios (0:1, 1:1, 1:2, 1:3, 3:1, 2:1) to identify the optimal Smix (surfactant-co-surfactant mixture) ratio.

The emulsification efficiency was found to be closely related to the HLB (Hydrophilic-Lipophilic Balance) value of the surfactant. Based on ternary phase diagrams (TPDs), it was observed that: A 1:1 and 2:1 (Tween 80:Transcutol P) ratio progressively enhanced the nanoemulsion region. Further increasing Tween 80 in the Smix ratio reduced the nanoemulsion-forming area. Higher proportions of Transcutol P did not significantly improve nanoemulsion formation.

FTIR studies

Fourier-transform infrared spectroscopy was employed to characterize the functional groups of Luliconazole and formulation excipients. The pure drug spectrum displayed characteristic absorption bands at 722.11 cm^{-1} (C-Cl stretch), 2198.75 cm^{-1} (C≡N stretch), 3006.73 cm^{-1} (aromatic C-H stretch), 1554.81 cm^{-1} (aromatic C=C bending), and 941.33 cm^{-1} (C-S-C stretch). Transcutol P exhibited prominent peaks at 3429.09 cm^{-1} (O-H stretch), 1104.63 cm^{-1} (C-O-C stretch), and 2974.87 cm^{-1} (C-H stretch), while Tween 80 showed distinct absorptions at 1734.73 cm^{-1} (C=O stretch), 3475.26 cm^{-1} (O-H stretch), 1093.84 cm^{-1} (C-O-C stretch), and 2921.37 cm^{-1} (C-H stretch). The physical mixture spectrum maintained all fundamental vibrations with only minor shifts (720.56 cm^{-1} for C-Cl, 994.09 cm^{-1} for C-S-C, 3378.56 cm^{-1} for O-H, 2923.72 cm^{-1} for C-H, and 1095.98 cm^{-1} for C-O-C), confirming the absence of chemical interactions. The preservation of characteristic peaks without appearance of new bands demonstrates excellent compatibility between Luliconazole and the surfactant system (Transcutol P/Tween 80), indicating their suitability for pharmaceutical formulation development. The observed spectral patterns suggest only weak physical associations exist between components, without compromising the drug's chemical integrity.

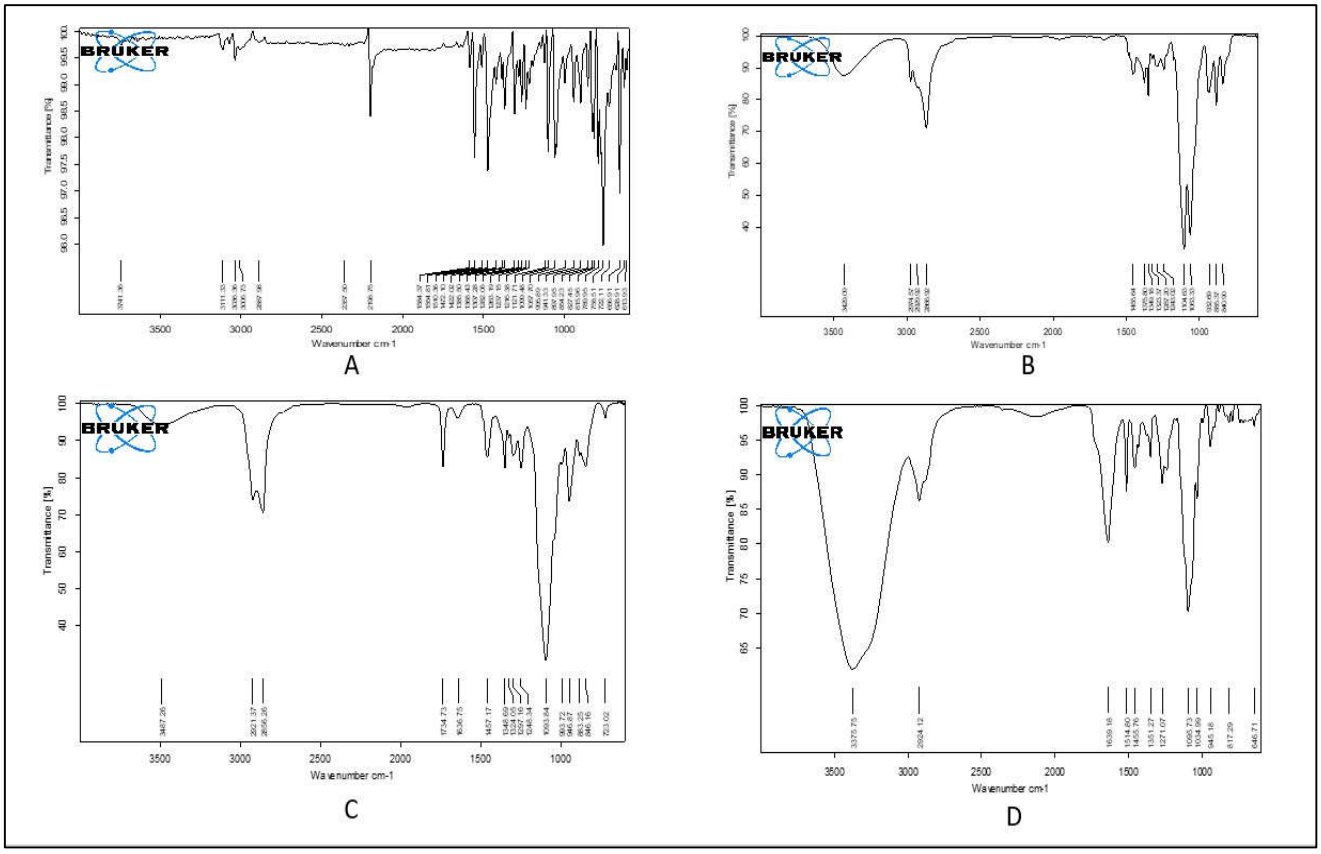

Fig. 3: (A) FTIR of pure luliconazole (B) FTIR of Transcutol P (C) FTIR of Tween 80 (D) FTIR of physical mixture of drug and surfactants

Optimization of nanoemulsions

The Design of Experiments (DoE) approach was implemented to systematically optimize the nanoemulsion formulations. A linear model was employed, generating 17 experimental batches with varying concentrations of oil (%), surfactant, and sonication time. The nanoemulsions were prepared by homogenizing the oil phase with the aqueous phase, followed by ultrasonication at predetermined intensity levels.

All formulations were evaluated for critical quality attributes, including globule size and entrapment efficiency. The Box-Behnken Design (BBD) experimental trials revealed that the nanoemulsions exhibited a globule size range of 72.3–172.3 nm, while the entrapment efficiency varied between 69.3% and 92.2% (Table 5). These results demonstrate the influence of the selected independent variables (oil concentration, surfactant ratio, and sonication time) on the formulation characteristics, highlighting the effectiveness of the DoE approach in optimizing nanoemulsion performance.

Effect of globule size on independent factors

The surface plot analysis revealed distinct trends in globule size variation with different formulation parameters. Increasing oil concentration (% v/v) consistently resulted in larger globule sizes, while elevation of the Smix ratio similarly led to gradual particle size augmentation (Fig. 4). However, statistical analysis indicated that neither oil concentration nor Smix ratio significantly influenced globule size ($p > 0.05$). Further examination (Fig. 5) demonstrated that prolonged sonication time initially caused a marginal size increase, followed by sustained reduction in particle dimensions. This biphasic response suggests that sonication duration exerted the most pronounced effect on globule size among the evaluated parameters, exhibiting greater impact than either oil content or surfactant mixture ratio. The observed pattern implies that extended ultrasonication effectively disrupts emulsion droplets, ultimately yielding smaller, more uniform nanoparticles despite the transient initial size increase.

Table 5: Luliconazole nanoemulsion experimental batches with glouble size (nm) and entrapment efficiency (%) results

Std	Factor 1	Factor 2	Factor 3	Response 1	Response 2
	A: Oil	B: Smix	C: Sonication time	Globule size	EE
	% V/V	% V/V	Min	Nm	%
1	5	15	10	117.4±1.12	76.5±1.46
2	15	15	10	166.8±1.26	92.2±2.27
3	5	45	10	147.2±2.15	78.6 ±1.64
4	15	45	10	126.4±2.22	78.9±2.33
5	5	30	5	141.7±1.18	82.4±1.57
6	15	30	5	172.3± 1.15	78.9± 2.46
7	5	30	15	85.3±1.20	69.3±2.54
8	15	30	15	78.4±1.15	90.6±2.66
9	10	15	5	168.4±2.26	88.4±1.53
10	10	45	5	136.4±1.23	77.5±1.48
11	10	15	15	72.3±2.13	77.7±1.58
12	10	45	15	95.3±1.47	85.6±0.73
13	10	30	10	142.9±1.32	76.9±1.64
14	10	30	10	136±1.25	82.4±2.53
15	10	30	10	140.2±2.13	83.9±1.48
16	10	30	10	144.2±2.19	81.8±1.62
17	10	30	10	137.7±1.27	82.5±2.52

Results are expressed in mean±SD (n=3)

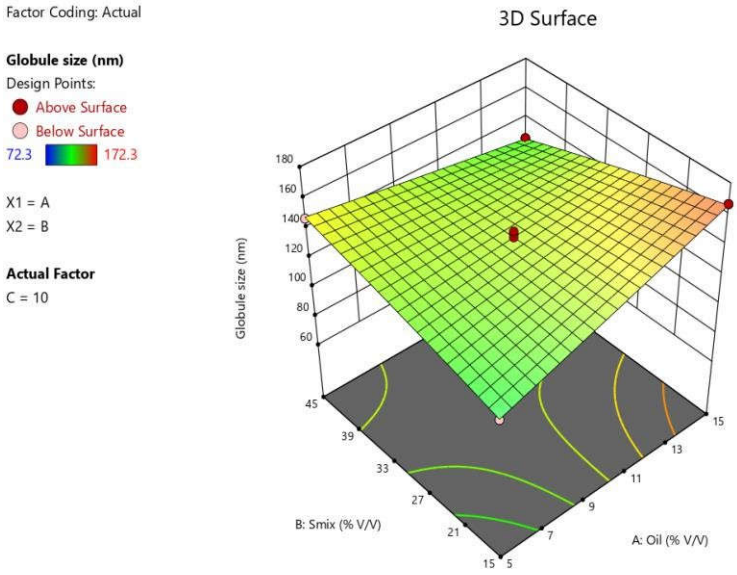

Fig. 4: 3D Surface plot of globule size against oil (%v/v) and Smix

Effect of % entrapment efficiency on independent factors

The 3D response surface analysis (Fig. 6) demonstrated that both Smix ratio and oil concentration significantly affected drug entrapment efficiency. While increasing the Smix ratio produced modest improvements in encapsulation, elevating the oil content (% v/v) resulted in substantially greater enhancement of entrapment efficiency. These findings indicate that the oil phase concentration served as the dominant factor governing drug incorporation within the nanoemulsion system.

Further optimization studies (Fig. 7) revealed that prolonged sonication time progressively improved entrapment efficiency, though to a lesser extent than oil concentration variations. The combined analysis established that both sonication duration and oil content significantly contributed to achieving optimal drug loading, with oil concentration exhibiting particularly strong positive correlation with encapsulation performance. These results provide critical formulation insights, demonstrating that careful balancing of these key parameters can effectively maximize the drug payload in nanoemulsion systems.

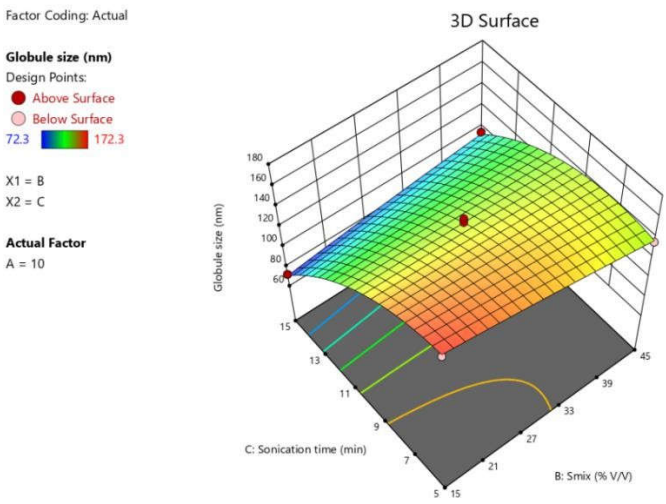

Fig. 5: 3D surface plot of globule size against sonication time and Smix

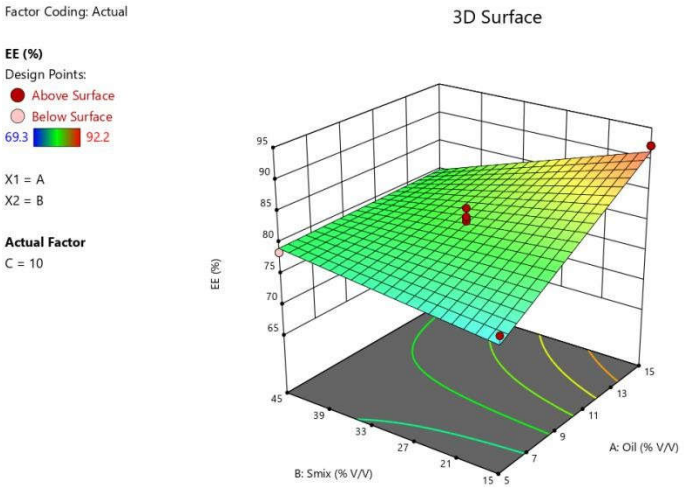

Fig. 6: 3D Surface plot of entrapment efficiency (%) against oil (%v/v) and Smix

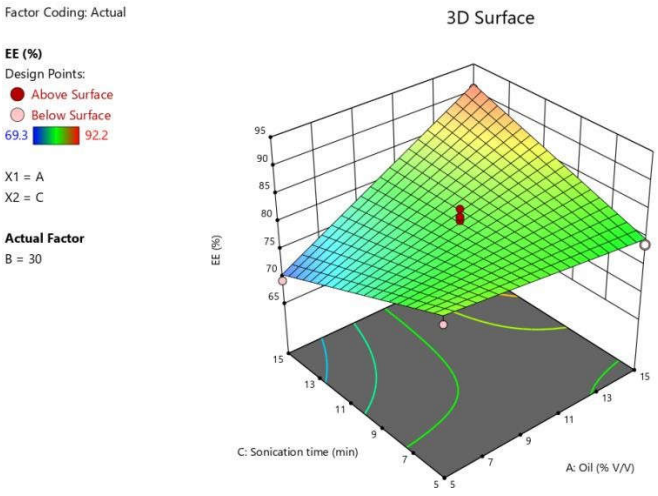

Fig. 7: 3D Surface plot of entrapment efficiency (%) against sonication time and oil (%v/v)

Percentage error between predicted and observed values

The optimized Luliconazole nanoemulgel demonstrated a mean globule size of 130.5 nm and an entrapment efficiency of 80%. Both the globule size and entrapment efficiency in the optimized nanoemulsion were within a ±5% margin of error compared to the predicted values. The findings were statistically significant at a 95% confidence level, indicating strong reliability. Table 6 displays the selected solution along with the percentage error between the predicted and observed results for the evaluated factors.

Table 6: Selected solution and the % error between the predicted and observed values

Factors	**Responses**			
A: Oil (% v/v)	**B: Surfactant (% v/v)**	**C: Sonication time (min)**	**Globule size (nm)**	**Drug entrapment (%)**
Predicted values				
15%	**45%**	**10 min**	**134.42**	**78.16**
Actual values				
–	**–**	**–**	**130.5 ± 3.23**	**80 ± 1.43**

Error (%)				
–	–	–	**3.28**	**2.30**

±SD (n=3) represented as mean of 3 values

Globule size and polydispersibility index (PDI) of optimized formulation

The optimized Luliconazole nanoemulgel exhibited a mean globule size of 130.5 ± 3.23 nm and a polydispersity index (PDI) of 0.263 ± 2.67 (Fig. 8), confirming its nanoscale range. The PDI value below 0.3 suggested a monodisperse distribution with no signs of precipitation or phase separation. According to literature, nanoemulgels with particle sizes below 200 nm are ideal for topical drug delivery, as their smaller globule size enhances skin permeation, ensuring effective localized treatment. Additionally, such formulations can overcome systemic challenges like the first-pass effect, making them a promising approach for transdermal drug delivery [18].

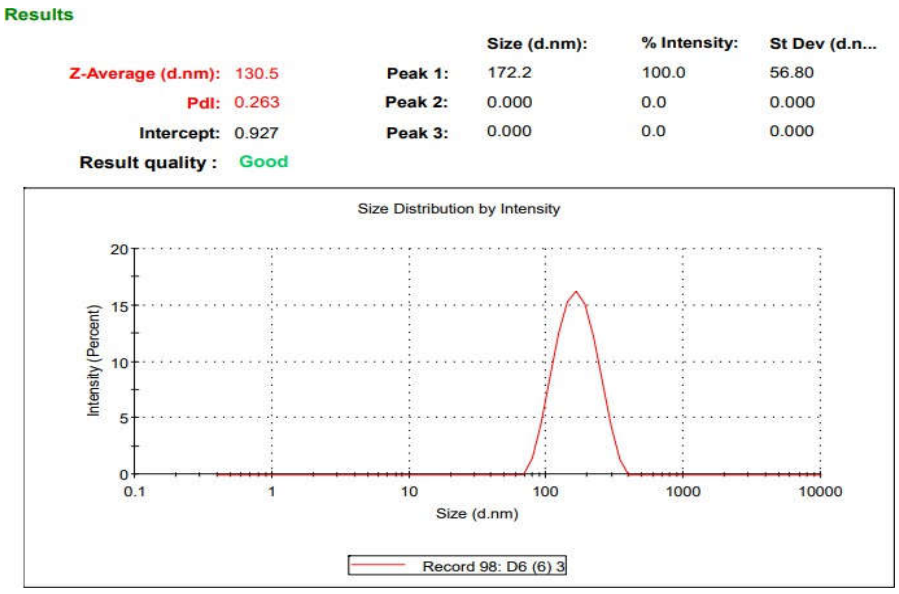

Fig. 8: Globule size and PDI of optimized formulation

Zeta potential measurement

Zeta potential is a critical factor influencing the stability and performance of nanoformulations. Studies suggest that nanoemulgels with zeta potential values between ±20-40 mV exhibit

enhanced stability due to strong electrostatic repulsion between similarly charged particles, preventing agglomeration and maintaining Brownian motion [20]. The optimized formulation in this study demonstrated a zeta potential of -21 ± 2.35 mV (Fig. 9), falling within the acceptable range for nanoemulsions, thereby ensuring good physical stability without significant fluctuations. This negative charge can be attributed to the anionic surfactants used in the formulation. Furthermore, nanoemulgels typically exhibit a more negative zeta potential compared to nanoemulsions, owing to the presence of carbopol's carboxylate groups, which contribute additional negative charges during gelling [12]. Despite the negative surface charge, the formulation remained stable, confirming that the measured zeta potential was sufficient to prevent particle aggregation and ensure long-term stability.

Transmission electron microscopy (TEM) analysis

Transmission Electron Microscopy (TEM) was employed to examine the morphological characteristics of the optimized nanoemulgel formulation. The TEM images (Fig. 10) confirmed the presence of uniform, spherical droplets with a smooth surface and an average size of approximately 100 nm, which correlated closely with the particle size measurements obtained from Malvern Zeta Sizer analysis. These findings further validate the nanoscale uniformity and structural integrity of the formulation.

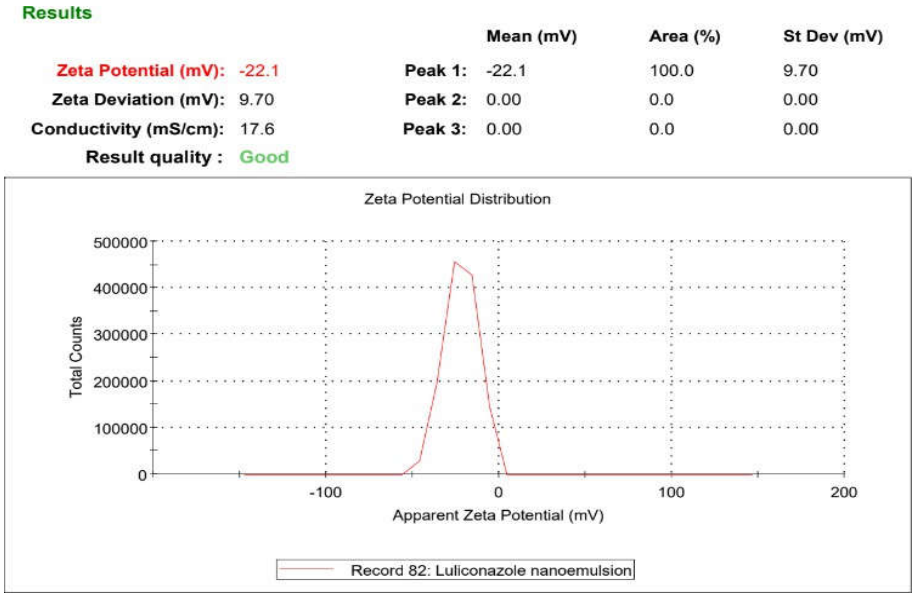

Fig. 9: Zeta potential data of optimized formulation

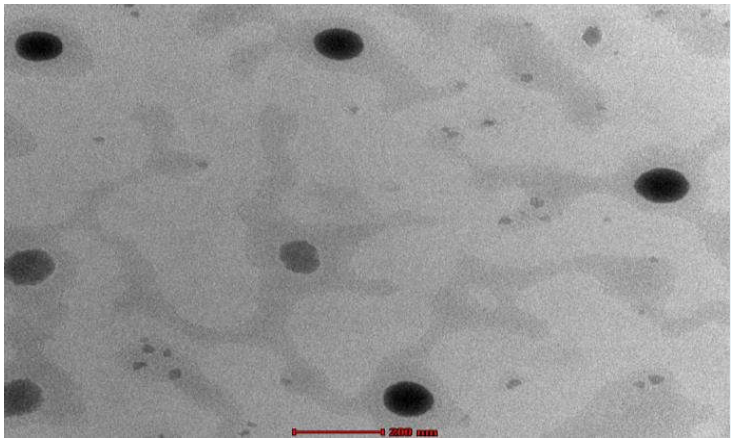

Fig. 10: TEM Image of optimized formulation

pH

pH evaluation serves as a critical quality attribute for topical formulations to ensure skin compatibility. The developed Luliconazole nanoemulgel exhibited a pH of 6.8 ± 2.25 (Table 5), well within the physiologically acceptable range (5.5–7.4) for dermatological applications. This near-neutral pH confirms the formulation's suitability for safe and non-irritating topical use, aligning with skin's natural pH balance.

Spreadability

The optimized Luliconazole nanoemulgel demonstrated excellent spreadability (13 ± 2.43 g·cm/sec, Table 5), ensuring effortless application due to its low resistance during spreading. The formulation exhibited a viscosity range of 378–5,640 cps, well within the ideal limits (50–50,000 cps) for semisolid dosage forms. Rheological analysis further confirmed its shear-thinning behavior, as evidenced by a pseudoplastic flow pattern—where increasing shear rate reduced viscosity, characteristic of non-Newtonian fluids. This property enhances patient compliance by facilitating smooth application while maintaining structural stability at rest.

Table 7: Results of pH, spreadability and drug content (%) for luliconazole nanoemulgel

shear, indicating that it has good spreadability.

% Drug content

‘

Evaluation Parameters of Optimized Luliconazole Nanoemulgel

Parameter	**Result**
pH	6.8 ± 2.25
Spreadability (g·cm/sec)	13 ± 2.43
Drug Content (%)	94.6 ± 1.9

Drug Content and Viscosity Analysis of Luliconazole Nanoemulgel

Drug Content Analysis

The optimized Luliconazole nanoemulgel demonstrated excellent drug content of 94.6 ± 1.9% (Table 7), confirming both content uniformity and homogeneous distribution throughout the formulation. This high percentage of active pharmaceutical ingredient (API) ensures consistent therapeutic efficacy, a critical quality attribute for semi-solid dosage forms.

Viscosity Profile

The rheological properties were evaluated using a Brookfield viscometer, with results showing viscosity values dependent on the formulation's oil and surfactant concentrations (Fig. 11). All measurements were performed in triplicate, with data expressed as mean ± standard deviation (n=3).

***In vitro* drug release study**

The *in vitro* drug release study of the formulated Luliconazole nanoemulgel was conducted for 8 h, during which the formulation showed a release rate of 74.93%±0.8% (fig. 12). Initially, there was a burst release within the first hour, which could be attributed to the presence of free drug adsorbed on the surface of the gel. As time progressed, there was a sustained release, possibly due to the lipophilic membrane entrapped within the gelling system. This led to the confirmation that the drug was released in a sustained manner over an extended period.

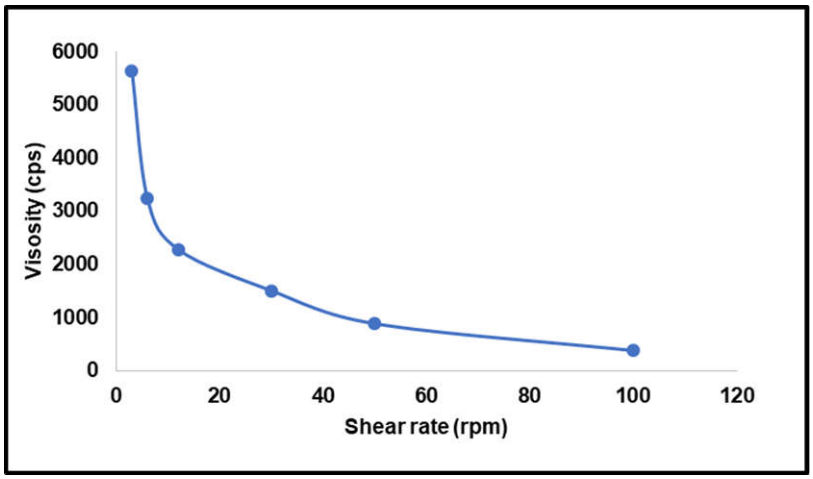

Fig. 11: Rheogram of optimized luliconazole nanoemulgel

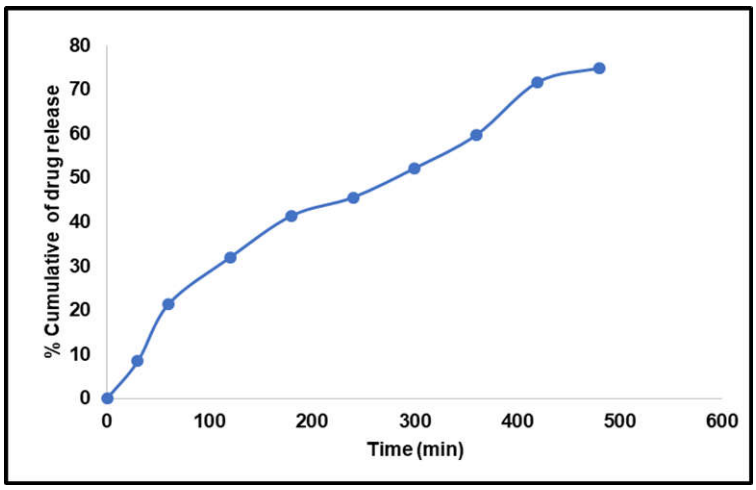

Fig. 12: Drug release profile of luliconazole-loaded nanoemulgel

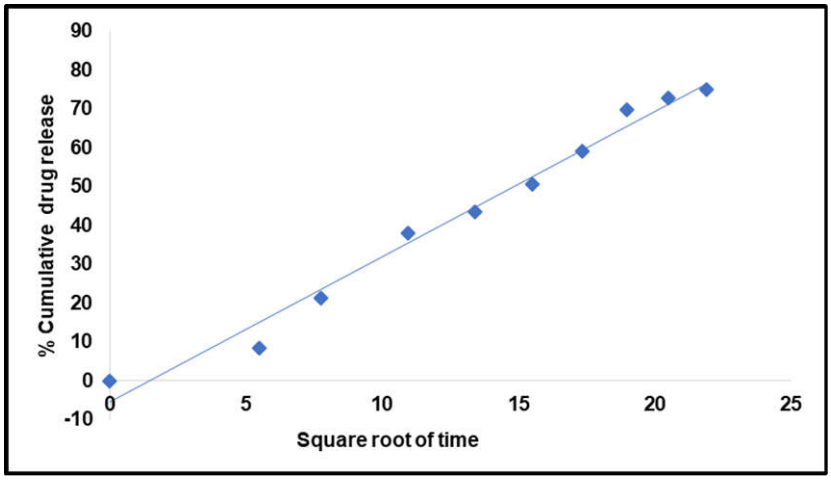

Fig. 13: Higuchi release kinetics model of Luliconazole loaded nanoemulgel

Drug release kinetics

The drug release profile of the optimized nanoemulgel formulation was systematically evaluated using various kinetic models, with particular emphasis on regression coefficient analysis. The results demonstrated excellent linearity (R^2 = 0.9828) for the Higuchi kinetic model (Fig. 13), strongly indicating a diffusion-controlled release mechanism. This finding suggests that drug liberation from the formulation occurs primarily through a combination of polymer matrix swelling and subsequent diffusion processes, characteristic of hydrogel-based delivery systems. The high correlation coefficient further confirms the predominance of this release mechanism in the developed nanoemulgel.

Conclusion

This study successfully developed and optimized a luliconazole-loaded nanoemulgel using a systematic Design of Experiments (DoE) approach to overcome the limitations of conventional antifungal formulations, such as poor solubility and inadequate skin permeation. The Box-Behnken Design (BBD) enabled precise optimization of key parameters—oil concentration (clove oil, 15% v/v), surfactant mixture (Tween 80:Transcutol P, 45% v/v), and sonication time (10 min)—resulting in a stable, nanoscale formulation with a globule size of 130.5 ± 3.23 nm, low PDI (0.263 ± 2.67), and high entrapment efficiency (80 ± 1.43%).

Physicochemical characterization confirmed the formulation's colloidal stability (zeta potential: -21 ± 2.35 mV), spherical morphology (TEM imaging), and pH compatibility (6.8 ± 2.25), ensuring suitability for topical application. The pseudoplastic rheological behavior and excellent spreadability (13 ± 2.43 g·cm/sec) further enhanced patient compliance. In vitro drug release studies demonstrated sustained release (74.93 ± 0.8% over 8 hours), following Higuchi kinetics (R^2 = 0.9828), indicating a diffusion-controlled mechanism. FTIR spectroscopy verified the absence of drug-excipient interactions, preserving luliconazole's structural integrity.

The developed nanoemulgel represents a significant advancement in topical antifungal therapy, offering enhanced solubility, improved skin permeation, and prolonged drug release compared to conventional formulations. Future studies should focus on in vivo efficacy, skin irritation tests, and clinical translation to validate its therapeutic potential for treating superficial fungal infections.

References

1. Acosta J. N., Falcone G. J., Rajpurkar P., Topol E. J. (2022). Multimodal biomedical AI. Nat. Med. 28 (9), 1773–1784. 10.1038/s41591-022-01981-2
2. Alicea G. M., Rebecca V. W., Goldman A. R., Fane M. E., Douglass S. M., Behera R., et al. (2020). Changes in aged fibroblast lipid metabolism induce age-dependent melanoma cell resistance to targeted therapy via the fatty acid transporter FATP2. Cancer Discov. 10 (9), 1282–1295. 10.1158/2159-8290.cd-20-0329
3. An Y., Zhu J., Liu F., Deng J., Meng X., Liu G., et al. (2019). Boosting the ferroptotic antitumor efficacy via site-specific amplification of tailored lipid peroxidation. ACS Appl. Mater. interfaces 11 (33), 29655–29666. 10.1021/acsami.9b10954
4. Anderson N. R., Minutolo N. G., Gill S., Klichinsky M. (2021). Macrophage-based approaches for cancer immunotherapy. Cancer Res. 81 (5), 1201–1208. 10.1158/0008-5472.CAN-20-2990
5. Anstensrud A. K., Molden E., Haug H. J., Qazi R., Muriq H., Fosshaug L. E., et al. (2020). Impact of genotype-predicted CYP2D6 metabolism on clinical effects and tolerability of metoprolol in patients after myocardial infarction – a prospective observational study. Eur. J. Clin. Pharmacol. 76 (5), 673–683. 10.1007/s00228-020-02832-0
6. Bajza Á., Kocsis D., Berezvai O., Laki A. J., Lukács B., Imre T., et al. (2020). Verification of P-glycoprotein function at the dermal barrier in diffusion cells and dynamic "Skin-On-A-Chip" microfluidic device. Pharmaceutics 12 (9), 804. 10.3390/pharmaceutics12090804
7. Barbero A. M., Frasch H. F. (2006). Transcellular route of diffusion through stratum corneum: results from finite element models. J. Pharm. Sci. 95 (10), 2186–2194. 10.1002/jps.20695
8. Barkve T. F., Langseth-Manrique K., Bredesen J. E., Gjesdal K. (1986). Increased uptake of transdermal glyceryl trinitrate during physical exercise and during high ambient temperature. Am. heart J. 112 (3), 537–541. 10.1016/0002-8703(86)90518-1
9. Baroni A., Buommino E., De Gregorio V., Ruocco E., Ruocco V., Wolf R. (2012). Structure and function of the epidermis related to barrier properties. Clin. dermatology 30 (3), 257–262. 10.1016/j.clindermatol.2011.08.007

10. Barrera J. B., Gijsen H., González A., De Groot A., Prota G., Wijnberg J., et al. (1995). The chemistry of melanins and melanogenesis. Fortschritte der chemie organischer naturstoffe/progress Chem. Org. Nat. Prod. 64, 93–148. 10.1007/978-3-7091-9337-2_2

11. Baryakova T. H., Pogostin B. H., Langer R., McHugh K. J. (2023). Overcoming barriers to patient adherence: the case for developing innovative drug delivery systems. Nat. Rev. Drug Discov. 22 (5), 387–409. 10.1038/s41573-023-00670-0

12. Bera K., Braman N., Gupta A., Velcheti V., Madabhushi A. (2021). Predicting cancer outcomes with radiomics and artificial intelligence in radiology. Nat. Rev. Clin. Oncol. 19 (2), 132–146. 10.1038/s41571-021-00560-7

13. Bhar S., Zhao G., Bartel J. D., Sterchele H., Del Mazo A., Emerson L. E., et al. (2022a). Bacterial extracellular vesicles control murine norovirus infection through modulation of antiviral immune responses. Front. Immunol. 13, 909949. 10.3389/fimmu.2022.909949

14. Bhardwaj N., Kundu S. C. (2010). Electrospinning: a fascinating fiber fabrication technique. Biotechnol. Adv. 28 (3), 325–347. 10.1016/j.biotechadv.2010.01.004

15. Bhuptani R. S., Patravale V. B. (2019). Starch microsponges for enhanced retention and efficacy of topical sunscreen. Mater. Sci. Eng. C, Mater. Biol. Appl. 104, 109882. 10.1016/j.msec.2019.109882

16. Nikam, A. N., Roy, A., Raychaudhuri, R., Navti, P. D., Soman, S., Kulkarni, S., Shirur, K. S., Pandey, A., & Mutalik, S. (2024). Organogels: "GelVolution" in Topical Drug Delivery - Present and Beyond. *Current pharmaceutical design*, *30*(7), 489–518. https://doi.org/10.2174/0113816128279479231231092905

17. Zhao, L., Chen, J., Bai, B., Song, G., Zhang, J., Yu, H., Huang, S., Wang, Z., & Lu, G. (2024). Topical drug delivery strategies for enhancing drug effectiveness by skin barriers, drug delivery systems and individualized dosing. *Frontiers in pharmacology*, *14*, 1333986. https://doi.org/10.3389/fphar.2023.1333986

18. Lunter, D., Klang, V., Eichner, A., Savic, S. M., Savic, S., Lian, G., & Erdő, F. (2024). Progress in Topical and Transdermal Drug Delivery Research-Focus on Nanoformulations. *Pharmaceutics*, *16*(6), 817. https://doi.org/10.3390/pharmaceutics16060817

19. Brito, S., Baek, M., & Bin, B. H. (2024). Skin Structure, Physiology, and Pathology in Topical and Transdermal Drug Delivery. *Pharmaceutics*, *16*(11), 1403. https://doi.org/10.3390/pharmaceutics16111403

20. Nikam, A. N., Roy, A., Raychaudhuri, R., Navti, P. D., Soman, S., Kulkarni, S., Shirur, K. S., Pandey, A., & Mutalik, S. (2024). Organogels: "GelVolution" in Topical Drug Delivery - Present and Beyond. *Current pharmaceutical design*, *30*(7), 489–518. https://doi.org/10.2174/0113816128279479231231092905

21. Raina, N., Rani, R., Thakur, V. K., & Gupta, M. (2023). New Insights in Topical Drug Delivery for Skin Disorders: From a Nanotechnological Perspective. *ACS omega*, *8*(22), 19145–19167. https://doi.org/10.1021/acsomega.2c08016

22. Hmingthansanga, V., Singh, N., Banerjee, S., Manickam, S., Velayutham, R., & Natesan, S. (2022). Improved Topical Drug Delivery: Role of Permeation Enhancers and Advanced Approaches. *Pharmaceutics*, *14*(12), 2818. https://doi.org/10.3390/pharmaceutics14122818

23. Roberts, M. S., Cheruvu, H. S., Mangion, S. E., Alinaghi, A., Benson, H. A. E., Mohammed, Y., Holmes, A., van der Hoek, J., Pastore, M., & Grice, J. E. (2021). Topical drug delivery: History, percutaneous absorption, and product development. *Advanced drug delivery reviews*, *177*, 113929. https://doi.org/10.1016/j.addr.2021.113929

24. Umar, A. K., Butarbutar, M., Sriwidodo, S., & Wathoni, N. (2020). Film-Forming Sprays for Topical Drug Delivery. *Drug design, development and therapy*, *14*, 2909–2925. https://doi.org/10.2147/DDDT.S256666

25. Zhao, L., Chen, J., Bai, B., Song, G., Zhang, J., Yu, H., Huang, S., Wang, Z., & Lu, G. (2024). Topical drug delivery strategies for enhancing drug effectiveness by skin barriers, drug delivery systems and individualized dosing. *Frontiers in pharmacology*, *14*, 1333986. https://doi.org/10.3389/fphar.2023.1333986